

DESIGN, CONSTRUCTION, AND MTF TESTING OF
TWO PETZVAL-LIKE OBJECTIVE LENS SYSTEMS
USING A DOUBLE-PASS INTERFEROMETER AND
SLANTED EDGE

by

Samuel Kerin

Copyright © Samuel Kerin 2023

A Thesis Submitted to the Faculty of the

JAMES C. WYANT COLLEGE OF OPTICAL
SCIENCES

In Partial Fulfillment of the

Requirements For the Degree of

MASTER OF SCIENCE

In the Graduate College

THE UNIVERSITY OF

ARIZONA 2023

THE UNIVERSITY OF ARIZONA
GRADUATE COLLEGE

As members of the Master's Committee, we certify that we have read the thesis prepared by Samuel Kerin, titled "Design, Construction, and MTF Testing of Two Petzval-Like Objective Lens Systems Using a Double-Pass Interferometer and Slanted Edge" and recommend that it be accepted as fulfilling the dissertation requirement for the Master's Degree.

[Signature] Date: 11 August 2023
Professor David Brady

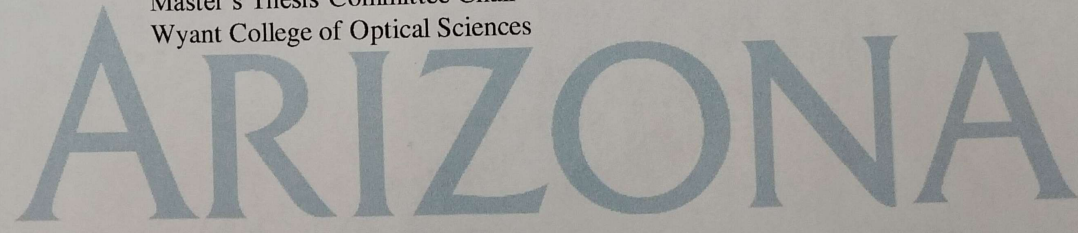
[Signature] Date: 11 August 2023
Professor Jose Sasian

[Signature] Date: 11 Aug 23
Professor Ron Driggers

Final approval and acceptance of this thesis is contingent upon the candidate's submission of the final copies of the thesis to the Graduate College.

I hereby certify that I have read this thesis prepared under my direction and recommend that it be accepted as fulfilling the Master's requirement.

[Signature] Date: 11 Aug 23
Professor David J. Brady
Master's Thesis Committee Chair
Wyant College of Optical Sciences



ACKNOWLEDGEMENTS

I would like to thank Professor David Brady for his guidance and help in the creation of this thesis. I would also like to thank Professor Jose Sasian for his own aid in guiding me through the process of testing and the theory of design behind these objectives. I would also like to thank my fellow students and coworkers who supported me throughout this process.

DEDICATION

To my parents, Peter and Nicole, and my siblings, Maggie and Lucas

TABLE OF CONTENTS

ABSTRACT.....	9
1. INTRODUCTION.....	10
1.1 Petzval Objective Design	10
2. DESIGN AND SPECIFICATIONS.....	11
2.1 Design goals	11
2.2 Ideal MTF and aberration performance	13
2.3 MTF performance with tolerancing	14
3. DOUBLE-PASS INTERFEROMETRY TESTING.....	17
3.1 Measurement with double-pass interferometer	17
3.2 Results	18
4. SLANTED-EDGE MTF TESTING	20
4.1 Method	20
4.2 Results	21
5. RECONCILIATION OF DIFFERENT MTF PERFORMANCE RESULTS BY METHOD ..	23
5.2 Improving Slanted Edge Test Performance.....	23
5.2 Simulating Error in Slanted Edge Test	26
5.3 Possible detector effects on MTF performance.....	28
5.4 Other potential factors	29
6. CONCLUSION.....	30
7. BIBLIOGRAPHY	31

LIST OF FIGURES

Figure 1: General design of a Petzval objective (Sasian, Joseph Petzval Lens Design Approach, 2017)	10
Figure 2: Surface diagram of the 25mm objective (left) and the 62.5 mm objective (right).....	11
Figure 3: MTF of the ideal 25 mm objective	13
Figure 4: MTF of the ideal 62.5 mm objective	14
Figure 5: MTF plots of 50 Monte Carlo tolerancing simulations of the 25 mm objective.....	16
Figure 6: MTF plots of 50 Monte Carlo Tolerancing Simulations of the 62.5 mm objective	16
Figure 7: Diagram of the WYKO 6000 double-pass Fizeau interferometer	17
Figure 8: An interferogram of one of the 25 mm objectives (left) and one of the 62.5 mm objectives (right)	18
Figure 9: MTF of the Zernike mean 62.5 mm objective.....	19
Figure 10: MTF of the Zernike mean 25 mm objective.....	19
Figure 11: Setup used for slanted edge MTF testing of the objectives	20
Figure 12: Full image of plywood slanted edge at 50 m imaged by the best 62.5 mm objective with region of interest highlighted (top) a zoom-in on the region of interest (middle) and the resulting MTF (bottom)	21
Figure 13: Full image of the slanted edge at 15 m imaged by the best 25 mm objective (top) a zoom-in on the region of interest (middle) and the resulting MTF (bottom)	22
Figure 14: Full image of printed slanted edge at 15 m imaged by the best-performing 25 mm objective (top-left) a zoom-in to show edge spread (top-right) and the resulting MTF (bottom)	25

Figure 15: Full image of printed slanted edge at 50 m imaged by the best-performing 62.5 mm objective (top-left) a zoom-in to show the edge spread (top-right) and the resulting MTF (bottom).....	26
Figure 16: Simulated slanted edge image of the 62.5mm objective (left) and resulting MTF (right)	27
Figure 17: Simulated slanted edge image of the 25 mm objective (left) and resulting MTF (right)	27
Figure 18: Simulated slanted edge image adjusted for the contrast of the real image of the 25 mm objective (left) and resulting MTF (right).....	28

LIST OF TABLES

Table 1: Surface data for the 62.5 mm objective	12
Table 2 Surface data for the 25 mm objective	12
Table 3: Seidel Aberration Coefficients on the image plane of the two objectives	14
Table 4: Performance Specifications for the monochrome detector used.....	20

ABSTRACT

In 2022, Professor Jose Sasian designed two different Petzval-like objective lens systems for use in a multi-camera array. One objective had a focal length of 62.5 mm, and the other had a focal length of 25 mm. These lens systems were designed with the goal of being diffraction-limited, having strong Modulation Transfer Function (MTF) performance, minimal aberrations, and being easy to construct. These systems were then tested with a double-pass interferometer and a slanted edge to measure their MTF performance. What was discovered was that the slanted edge testing indicated that the systems had far inferior MTF performance than the theoretical data and double-pass interferometer had indicated, falling much further short of diffraction-limited performance. Several explanations for this discrepancy were explored, such as potential detector effects, and methods of improving the quality of the slanted edge test were also implemented, but no conclusive cause for the discrepancy was able to be identified.

1. INTRODUCTION

1.1 Petzval Objective Design

Historically speaking, the Petzval Objective was the first photographic objective lens system to be deliberately designed from the ground up, rather than constructed from a prefabricated collection of lenses (Vasiljević, 2002). Initially constructed in 1841 by Joseph Maximillian Petzval as part of Voigtländer's early metal camera design, his eponymous objective lens system typically features a pair of widely-spaced achromatic doublets with the aperture stop at the rim of the first doublet. In a Petzval portrait objective, chromatic and spherical aberrations are corrected at each doublet, positive coma in the first doublet is corrected with negative coma in the second, and the negative astigmatism introduced by the negative coma of the second doublet is used as a means of artificially flattening the field of view (Sasian, Lecture 15: Refractive Systems, 2022). For Petzval-like objectives that still maintain a curved field of view, a final field-flattening lens can be added near the image plane to correct for any curvature that remains in the system.

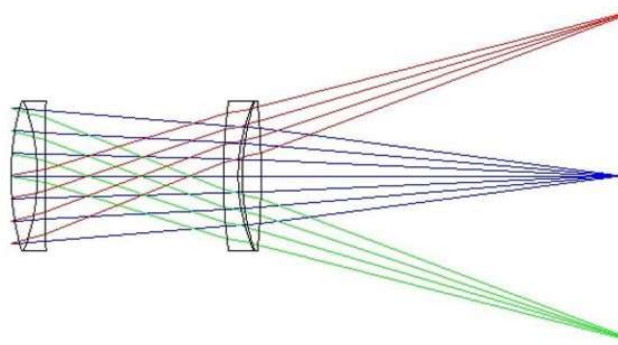


Figure 1: General design of a Petzval objective (Sasian, Joseph Petzval Lens Design Approach, 2017)

2. DESIGN AND SPECIFICATIONS

2.1 Design goals

The two objective designs that were tested were Petzval objectives with focal lengths of 25 mm and 62.5 mm. In designing and constructing these objectives, Professor Sasian stated that he had several goals. One primary objective of his design was to maximize the number of planar surfaces and avoid aspheric surfaces to simplify construction and reduce cost. Additionally, aberrations were minimized in order to achieve apochromaticism and provide strong MTF performance to ensure the objectives are diffraction-limited. Lastly, selective assembly was performed specifically to remove spherical aberration and as much uniform coma as possible. (Sasian, personal communication, May 22, 2023)

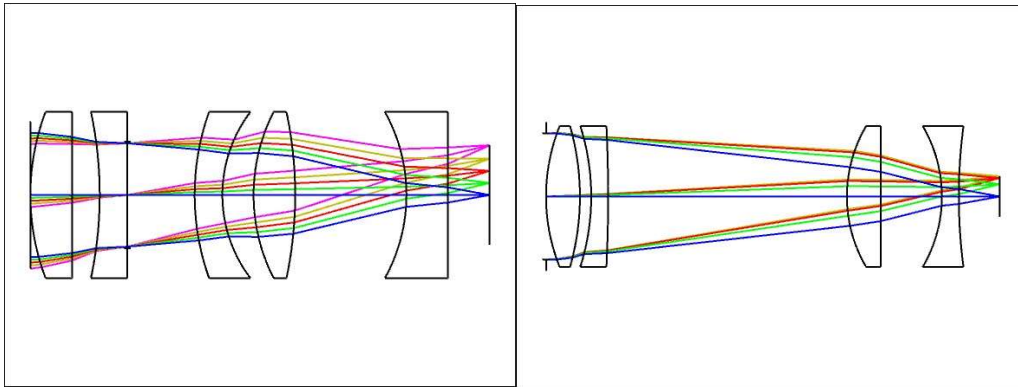


Figure 2: Surface diagram of the 25mm objective (left) and the 62.5 mm objective (right)

Surface	Radius of Curvature (mm)	Thickness (mm)	Glass
Stop	-	-	-
1	33.475	6.000	N-FK51A
2	-45.361	2.000	-
3	-41.313	3.000	N-LASF43
4	-258.212	42.329	-
5	24.572	6.000	N-SSK2
6	Infinity	10.830	-
7	-24.572	3.000	N-SF11
8	95.210	7.250	-
Image	-	-	-

Table 1: Surface data for the 62.5 mm objective

Surface	Radius of Curvature (mm)	Thickness (mm)	Glass
1	17.000	3.000	S-LAL18
2	Infinity	2.000	-
3	-28.835	2.000	S-TIH11
Stop	-	4.853	-
4	Infinity	42.329	-
5	17.830	2.000	S-TIH11
6	9.911	2.251	-
7	13.177	3.000	S-LAL18
8	-28.835	8.026	-
9	-12.341	3.000	S-LAL18
10	Infinity	3.000	-
Image	-	-	-

Table 2 Surface data for the 25 mm objective

Proper glass selection for each doublet was necessary to remove any chromatic aberration in the system. Spacing the doublets both from each other and internally offered another degree of freedom which corrected for aberrations within the objectives, allowed the surfaces inside each

doublet to be independent, and allowed for simpler surface shapes to be used while achieving nearly diffraction-limited performance. It can be observed from Figure 2 that a field-flattening lens was required behind the second doublet to correct for field curvature that was not already artificially flattened by the second doublet.

2.2 Ideal MTF and aberration performance

Making use of the lens design program Zemax OpticStudio, the theoretical performance of the Petzval Objective lenses can be analyzed. It is possible to obtain the Siedel aberration coefficients at the image plane, and, using the Fast Fourier Transform, a plot of the MTF of these Petzval objectives can be generated as well.

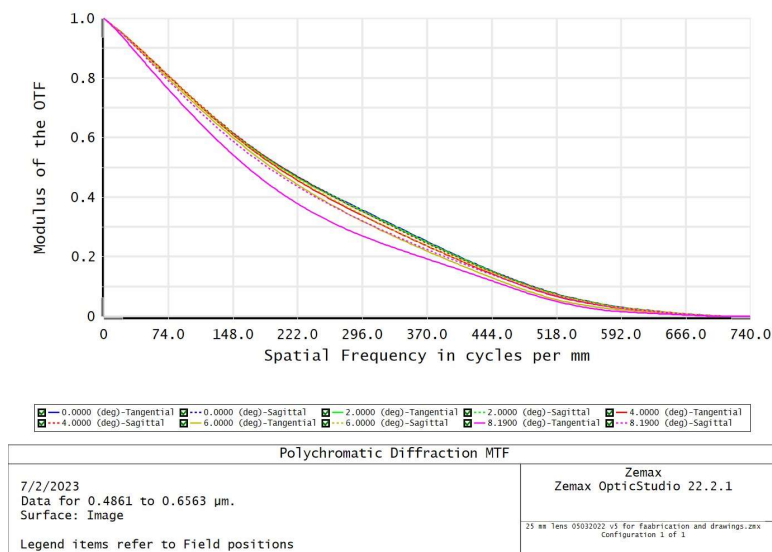


Figure 3: MTF of the ideal 25 mm objective

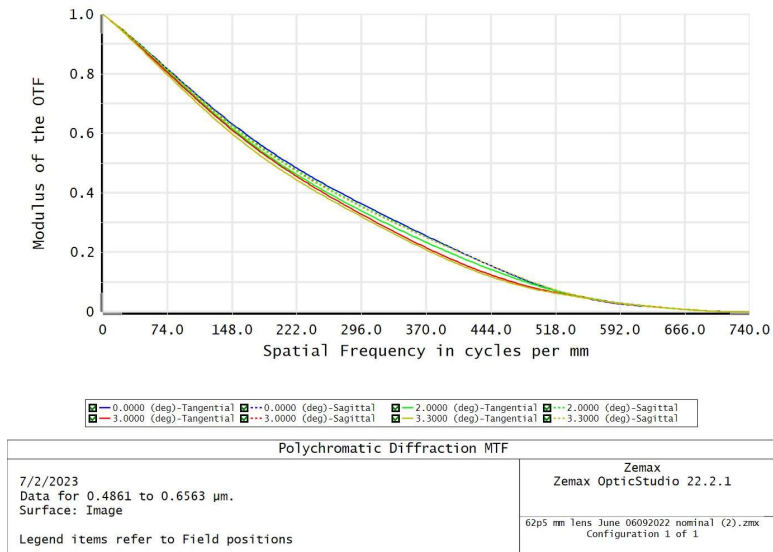


Figure 4: MTF of the ideal 62.5 mm objective

Aberration Coefficient	62.5 mm (waves)	25 mm (waves)
W040	0.595069	0.728062
W131	0.504437	0.130358
W222	-0.070821	0.264740
W220P	0.175925	0.387804
W311	0.050990	0.403075
W020	-0.576809	-0.377043
W111	-0.066787	0.238379

Table 3: Seidel Aberration Coefficients on the image plane of the two objectives
in units of waves of length $0.63288 \mu\text{m}$

2.3 MTF performance with tolerancing

In addition to finding the ideal performance of these objectives, a tolerance analysis was done in Zemax OpticStudio to obtain a broader spectrum of potential MTF performances that may result in imprecision in manufacturing. According to the tolerancing data given in the inspection data sheet provided by Salvo Technologies, the manufacturer of these objectives, the

lens wedge was made at an angle of less than 1 arc minute, so the tolerance for surface tilt was set to 1/2 arc-minutes. Additionally, element decenter tolerance was up to 0.0125 mm and thickness tolerance was about 0.025 mm. Lastly, the tolerance for the radii of curvature/power of the objectives was stated to be approximately 3 Newton rings. According to Professor Sasian, there were no tolerances for index of refraction and Abbe number due to the well-understood nature of the materials used in the objectives. Additionally, there was no tolerance surface decenter or radius, or element tilt.

A Monte Carlo simulation was run based on these given tolerance settings in order to analyze the MTF performance of the objectives for the given tolerance settings. This was done by doing 50 runs of the simulation while allowing Zemax OpticStudio to overlay the MTF plots for each run to see the range of possible MTF performances across these given tolerances. The RMS Wavefront criterion was selected as it was the criterion that best reflected the overall performance of the objectives under test. Additionally, the standard paraxial focus compensator was used, with a range of -2 mm to +2 mm. This is made to adjust the back focal distance in response to the random changes in the Monte Carlo simulation to ensure that best focus is maintained across all runs of the simulation.

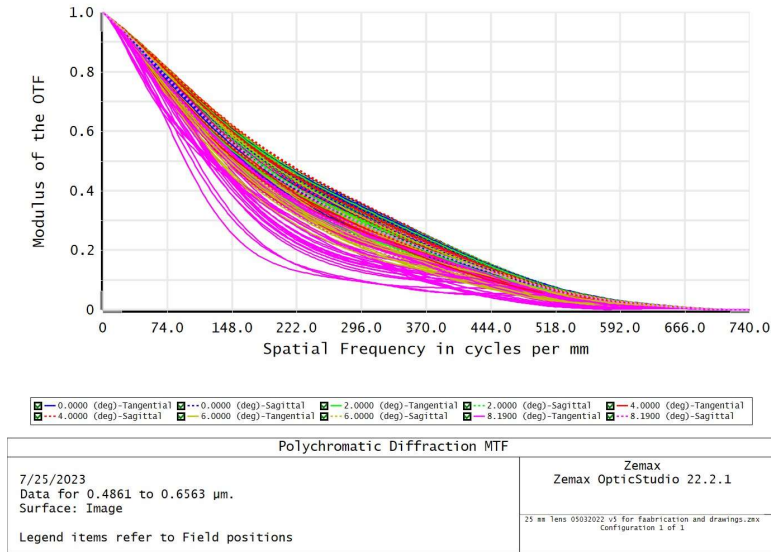


Figure 5: MTF plots of 50 Monte Carlo tolerancing simulations of the 25 mm objective

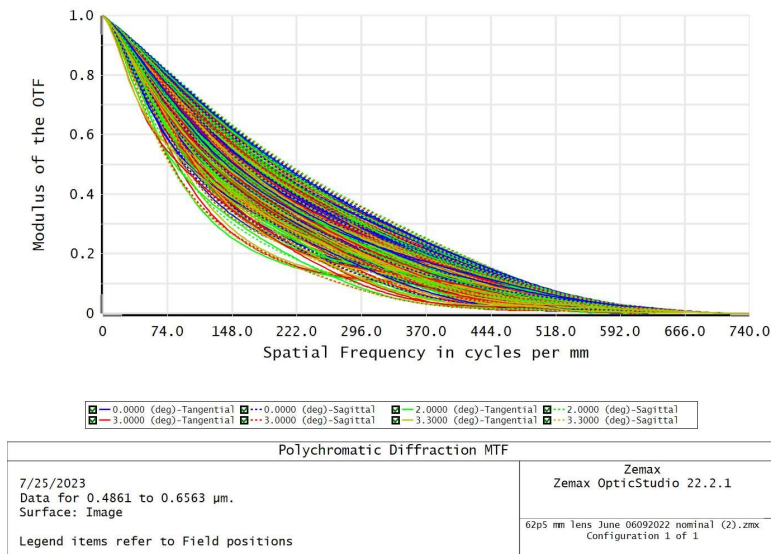


Figure 6: MTF plots of 50 Monte Carlo Tolerancing Simulations of the 62.5 mm objective

From Figures 6 and 7, it can be seen that there are many ways in which the objective's MTF performance may be significantly compromised within the given tolerances and fall far from diffraction-limited performance.

3. DOUBLE-PASS INTERFEROMETRY TESTING

3.1 Measurement with double-pass interferometer

The first method used to test the MTF performance of these lenses was with the use of a double-pass interferometer in order to measure surface deformities as well as any other causes of optical path difference that deviates from the expected design. This was done with a WYKO 6000 Double-Pass Fizeau Interferometer. The interferometer then provided a list of Zernike aberration coefficients that required a unit conversion from wavelengths of 632.8 nm to mm, and also needed to be divided by -2 due to the double-pass nature of this interferometer, which was done by Excel Spreadsheet. and were then uploaded to a Zemax OpticStudio file which simulated the whole interferometer system by modeling the Petzval Objectives as a Zernicke Fringe Sag, a mirrored surface placed twice the focal length of the lens under test away from the surface, with a focal length equivalent to the Petzval Objectives where the aberration coefficients provided by the interferometer are entered as parameters for the surface, normalized by the diameter of the lens tube under test.

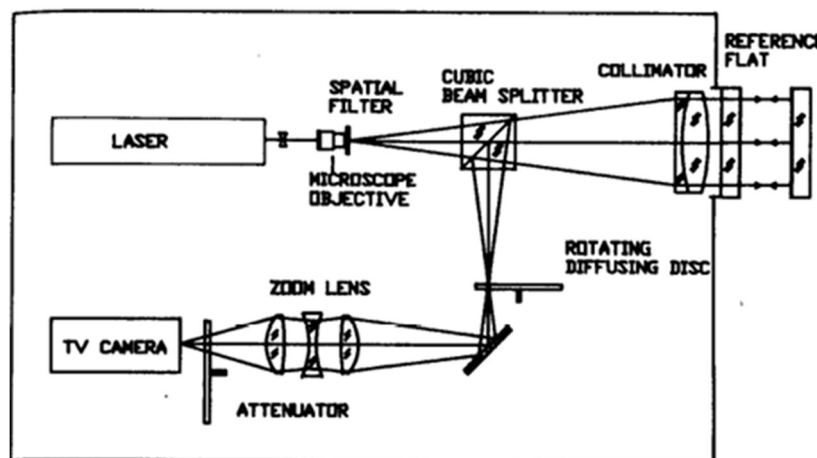


Figure 7: Diagram of the WYKO 6000 double-pass Fizeau interferometer

3.2 Results

The WYKO 6000 Fizeau Interferometer outputs an interferogram on a small display. These interferograms can be used to obtain a general understanding of the performance of the system. Overall, a diffraction-limited system will display a series of straight lines in its interferogram, and the straighter they are the closer the system is to being diffraction-limited.

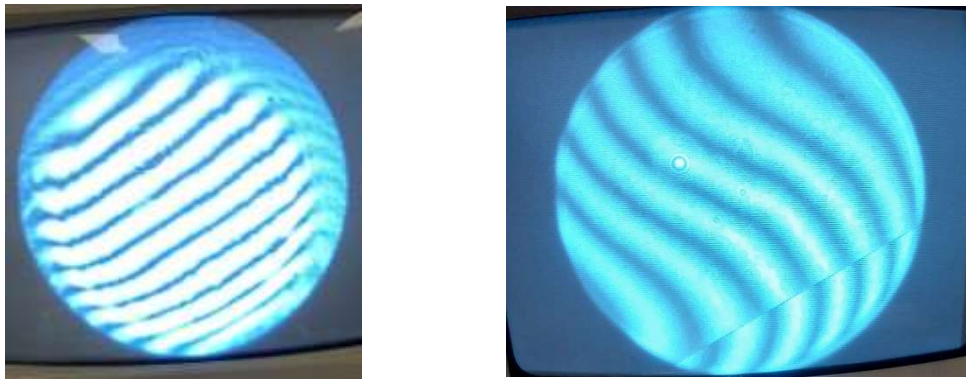


Figure 8: An interferogram of one of the 25 mm objectives (left) and one of the 62.5 mm objectives (right)

The interferograms here match a nearly diffraction-limited system, so there is an indication that these objectives will perform well.

The means of the Zernike coefficients measured for the 10 62.5 mm objectives and the 10 25 mm objectives were then calculated and imported into a Zemax file for analysis, resulting in the MTF plots displayed below.

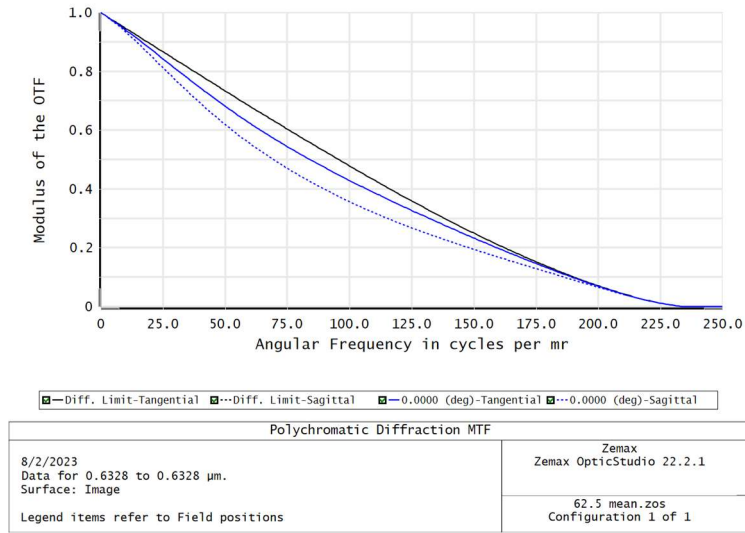


Figure 9: MTF of the Zernike mean 62.5 mm objective

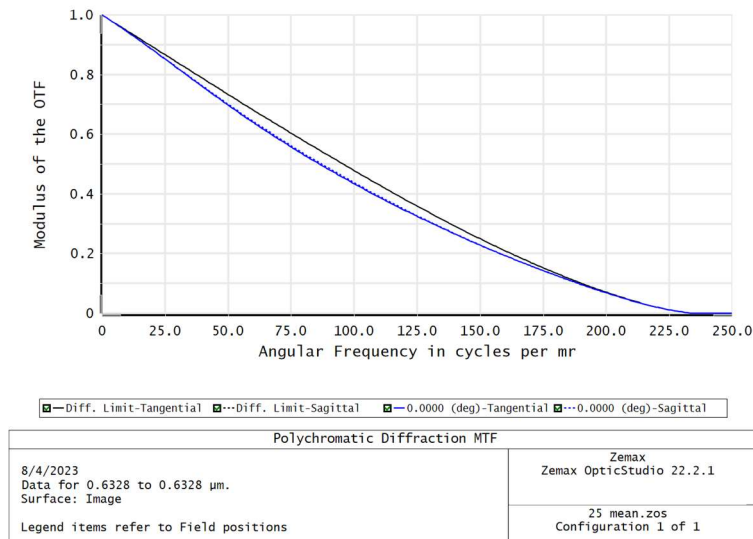


Figure 10: MTF of the Zernike mean 25 mm objective

Both of these plots indicate nearly diffraction-limited performance by the objectives, corroborating the theoretical MTF performance.

4. SLANTED-EDGE MTF TESTING

4.1 Method

The other method of testing these lens tubes was with a slanted edge test. This necessitated constructing a system to house the objectives and a slanted edge large enough to be visible at the ranges necessary for the testing.



Figure 11: Setup used for slanted edge MTF testing of the objectives

Performance Specifications

Model	VEN-830-22U3M/C
Interface	USB3.0
Resolution	3840(H) × 2160(V)
Frame rate	22 fps @3840 × 2160
Sensor	1/1.8", Rolling Shutter Sony IMX334 CMOS
Pixel size	2.0 μm × 2.0 μm
Pixel Bit Depth	8bit, 10bit
Spectrum	Monochrome / Color
Exposure time	20μs~1s

Table 4: Performance Specifications for the monochrome detector used

The images of the slanted edge were taken at a range of 50 m for the 62.5 mm objectives, and at 15 m for the 25 mm objectives. After the images were taken, they were then analyzed using the ImageJ plugin SE_MTF (Mitja, 2011).

4.2 Results

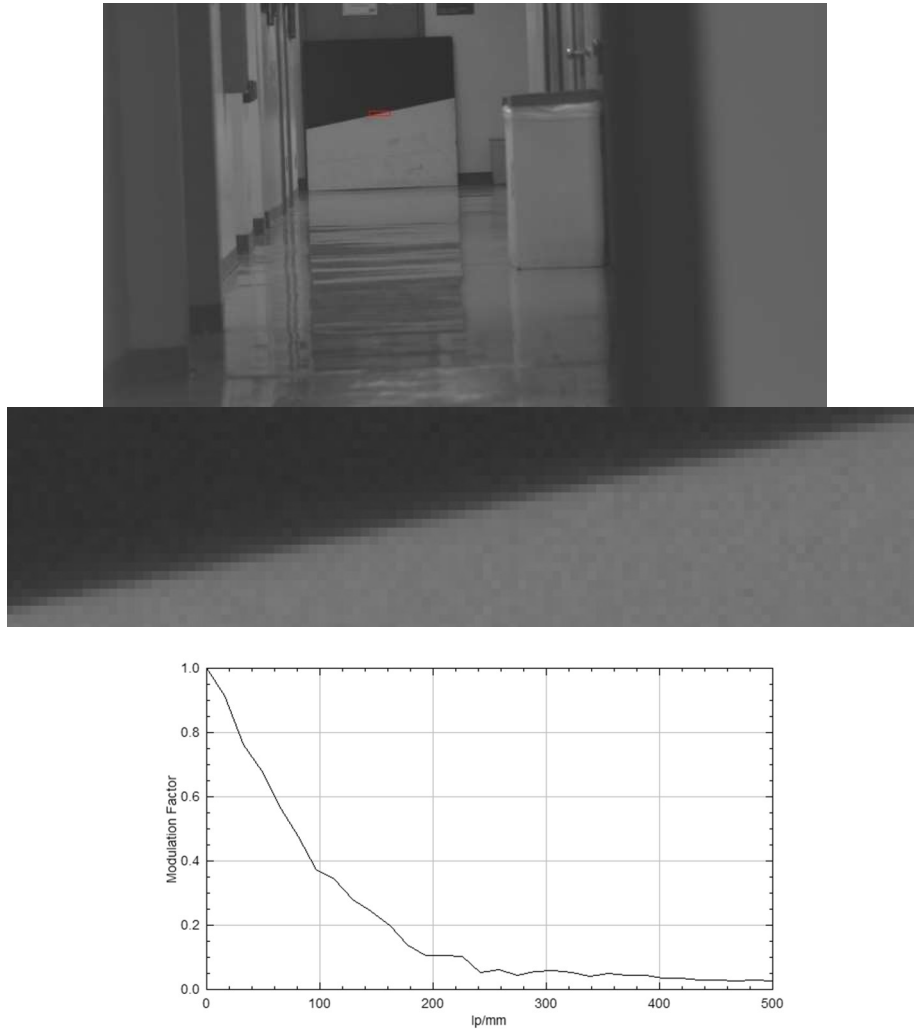


Figure 12: Full image of plywood slanted edge at 50 m imaged by the best 62.5 mm objective with region of interest highlighted (top) a zoom-in on the region of interest (middle) and the resulting MTF (bottom)

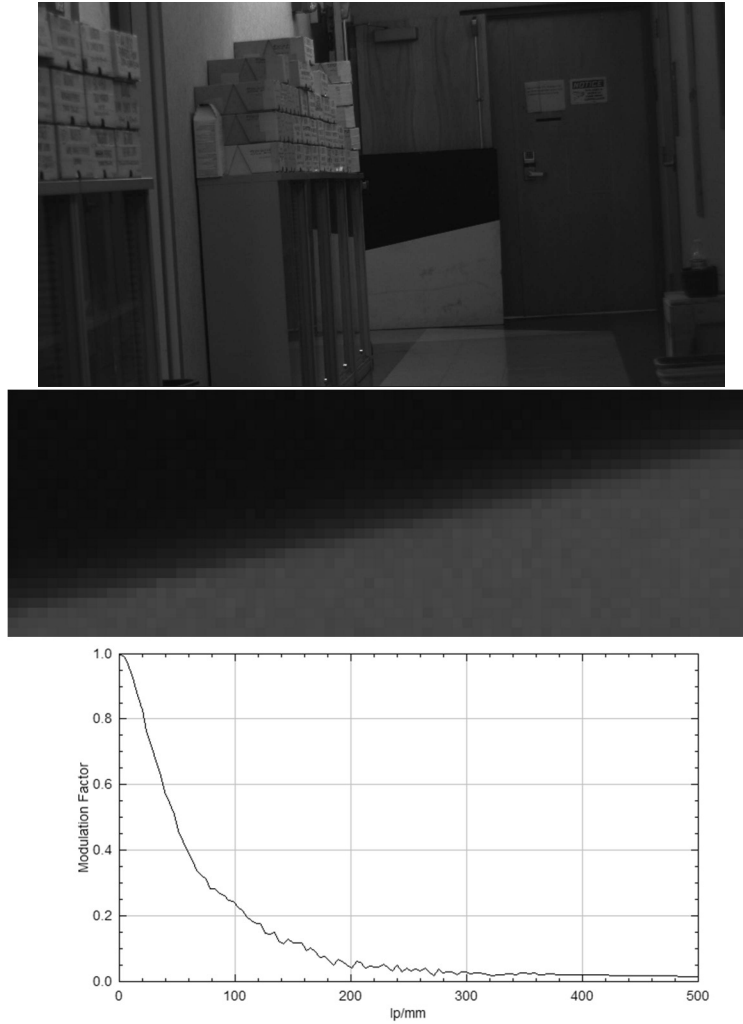


Figure 13: Full image of the slanted edge at 15 m imaged by the best 25 mm objective (top) a zoom-in on the region of interest (middle) and the resulting MTF (bottom)

This indicates that the MTF performances of these objectives are significantly below the theoretical performances, and far from the diffraction limit.

5. RECONCILIATION OF DIFFERENT MTF PERFORMANCE RESULTS BY METHOD

5.2 Improving Slanted Edge Test Performance

After the discrepancies between the theoretical performance, performance as measured in the interferometer, and performance as measured by the slanted edge test were found, attempts at improving the methodology of these measurements were made. Firstly, an improved version of the slanted edge MTF test was done, replacing the previous painted plywood edge, which had some significant imperfections when observed closely due to the nature of the paint and the rough surface of the plywood. It was found that for a slanted edge to provide a sufficient, the contrast transition of the edge target occurs of a scale four times smaller than the Nyquist limit (Edmund Optics, 2023). This would mean that for the 2 μm pixel size of the Daheng Imaging VEN-830-22U3M,

$$\textit{Transition Width}_{\textit{Image Space}} < \frac{\textit{Nyquist Width}}{4}$$

and since

$$\textit{Nyquist Width} = 2 * \textit{Pixel Width} = 4 \mu\text{m}$$

and

$$m * \textit{Transition Width}_{\textit{Object Space}} = \textit{Transition Width}_{\textit{Image Space}}$$

where m is the magnification of the system, this shows the required transition width of the target to be

$$\textit{Transition Width}_{\textit{Object Space}} < \frac{1 \mu\textit{m}}{m}$$

The magnification, m , can be approximated by dividing the focal length of each lens by the corresponding distance to the target. This gives

$$m_{25} \approx \frac{25\textit{mm}}{15\textit{m}} = 0.001\bar{6}, \quad m_{62.5} \approx \frac{62.5\textit{mm}}{50\textit{m}} = 0.00125$$

Which means that to be sufficient for both objectives, the target requires a transition width of

$$\textit{Transition Width}_{\textit{Object Space}} < 0.6\textit{mm}.$$

A casual observation of the target in question revealed that the edge imperfections brought on by smudges and imperfections in painting the edge led to the transition width far exceeding this limit. As such, a new slanted edge was printed onto a sheet of paper and used to conduct new tests.

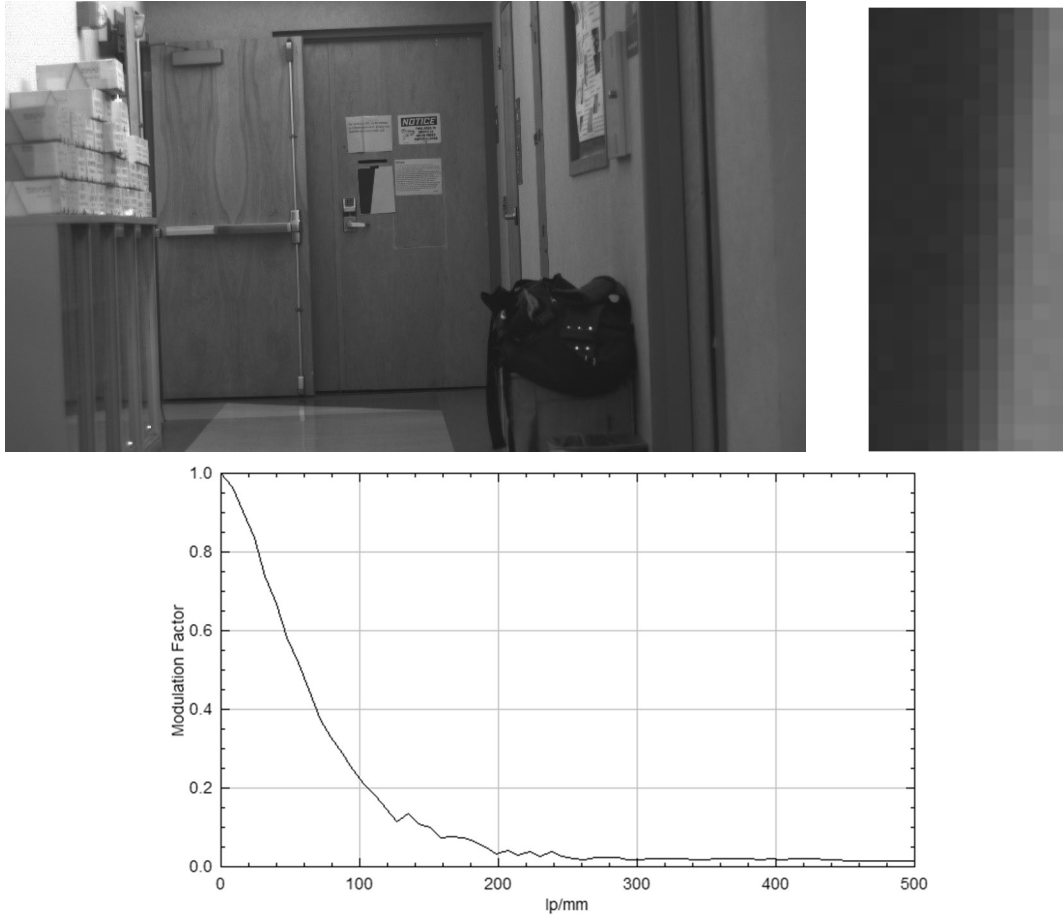


Figure 14: Full image of printed slanted edge at 15 m imaged by the best-performing 25 mm objective (top-left) a zoom-in to show edge spread (top-right) and the resulting MTF (bottom)

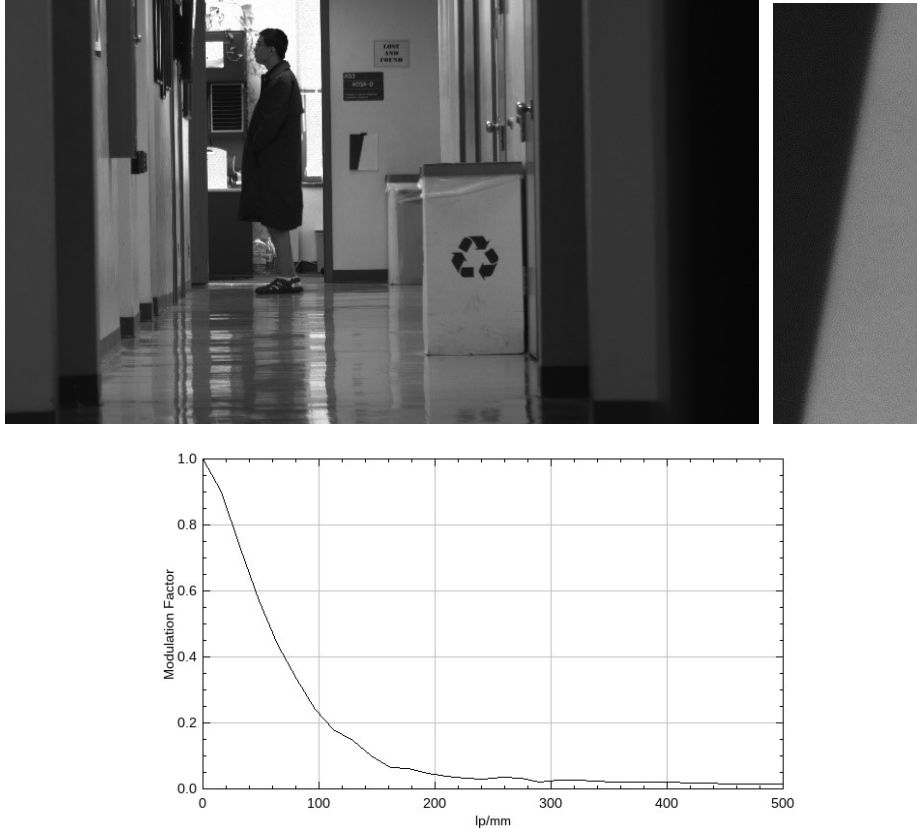


Figure 15: Full image of printed slanted edge at 50 m imaged by the best-performing 62.5 mm objective (top-left) a zoom-in to show the edge spread (top-right) and the resulting MTF (bottom)

Notably, there seems to be a significant drop in MTF performance when using the improved slanted edge. This would suggest that the precision of the slanted edge was not responsible for the poor MTF performance in these tests compared to the theoretical results and the interferometer data.

5.2 Simulating Error in Slanted Edge Test

Upon the discovery of this discrepancy, a theoretical model of the slanted edge MTF test was conducted in Zemax OpticStudio using the program’s “Extended Scene Analysis” tool which enables simulation of an image through an optical system using a specified detector size

and resolution. This was used to simulate how each objective would theoretically image a slanted edge onto a detector with the same properties as the one used. The resulting simulated images were then analyzed in ImageJ by the same method.

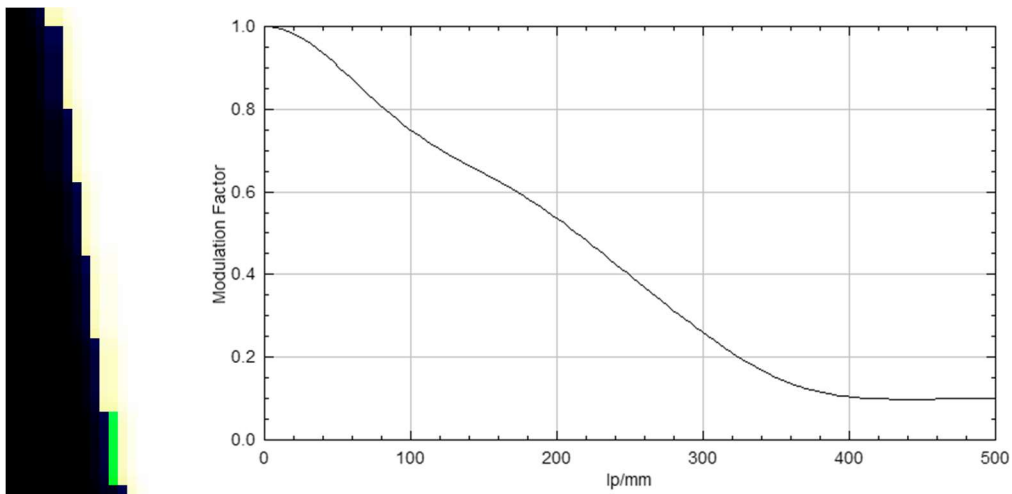


Figure 16: Simulated slanted edge image of the 62.5mm objective (left) and resulting MTF (right)

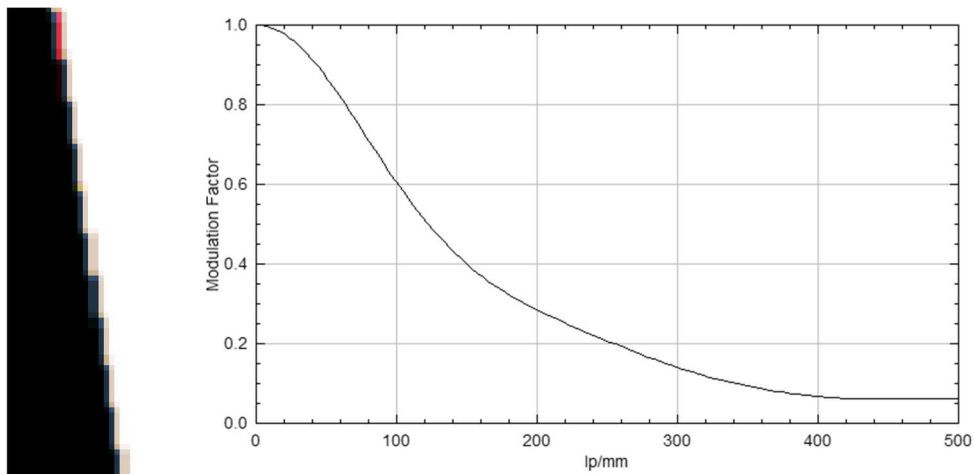


Figure 17: Simulated slanted edge image of the 25 mm objective (left) and resulting MTF (right)

Comparing the slanted edge images from figures 12 and 13 to these reveals that there must be some degree of error in the slanted edge test that was performed, and that had a negative

impact on the observed results. The much sharper image of the slanted edge in the simulated case indicates such. These are far closer to the theoretical results for the MTFs as well. However, using the contrast from the images of the slanted edge, we can account for any difference in contrast causing this discrepancy. ImageJ was used to analyze the contrast between the bright and dark regions of the slanted edge as imaged through the 25 mm objective. The dark region had a gray value of 43, and the bright region had a gray value of 125. Following this, a simulated slanted edge with bright and dark regions possessing those brightness values was created and also run through the image simulation program in Zemax.

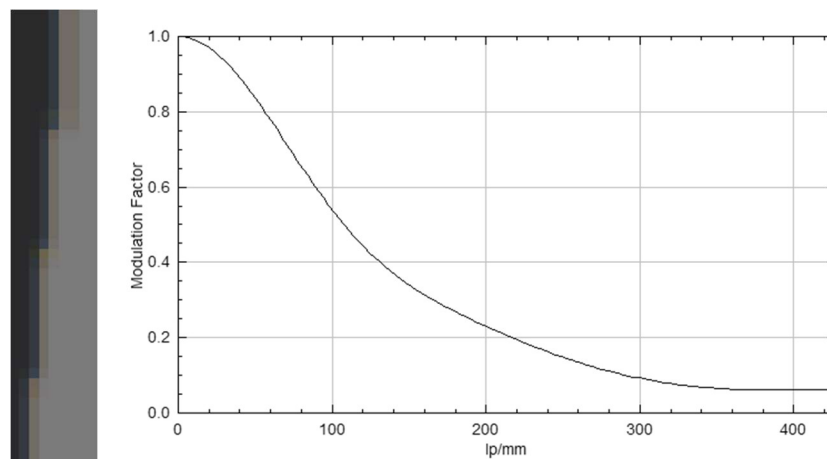


Figure 18: Simulated slanted edge image adjusted for the contrast of the real image of the 25 mm objective (left) and resulting MTF (right)

It seems clear that this is much closer in performance to the full-contrast slanted edge and does not significantly account for the discrepancy between it and the real image.

5.3 Possible detector effects on MTF performance

After improvements to the slanted edge test did not result in superior performance in the

slanted edge test, other metrics were necessary to determine the source of the discrepancy. One such hypothesis is that the system is being limited by the detector MTF. Theoretically, the detector MTF is the Fourier Transform of a 2-dimensional rectangle function. This would indicate that

$$MTF_{det} = |\text{sinc}(\xi w)|$$

Where w is the width of an individual pixel on the detector, which is $2 \mu\text{m}$. This would mean that the system becomes more detector-limited at higher spatial frequencies, above approximately 400 lines/mm, but this would not explain the significantly worse performance below that point. Additionally, since the Nyquist rate of the camera is 500 lines/mm, this also does not completely explain the poor performance below these frequencies.

5.4 Other potential factors

The error in the slanted edge MTF performance is significant. The typical difference between the theoretical MTF and measured MTF in a slanted edge test in the presence of noise is on average -4.88% (Xie, Fan, Wang, Wang, & Zou, 2018) so there may be some problem with the detector in use, the stability of the system, or the kinds of targets chosen. The possibility of turbulence effects playing a role was briefly considered, though at the selected ranges and temperatures indoors, this is more than likely not a significant factor in the poor MTF performance in this system. As of the conclusion of this report, the exact cause of the discrepancy has not been identified.

6. CONCLUSION

Ultimately, though the Fizeau interferometer testing corroborated the theoretically strong MTF and aberration performance of these Petzval objectives, the slanted edge test data did not indicate diffraction-limited performance in the same manner, and the difference in the expected and observed MTF performances greatly exceeded the expected error of a test such as this. Attempts to address this discrepancy by improving the quality of the slanted edge or accounting for other factors that may have caused this difference have not yielded a definitive explanation for this difference.

7. BIBLIOGRAPHY

- Edmund Optics. (2023, July 18). *Resolution and MTF Testing*. Retrieved from Edmund Optics Worldwide: <https://www.edmundoptics.eu/knowledge-center/application-notes/imaging/resolution-and-mtf-testing>
- Mitja, C. (2011, 11 31). *Slanted Edge MTF*. Retrieved from imagej.nih.gov: <https://imagej.nih.gov/ij/plugins/se-mtf/index.html>
- Sasian, J. (2017). Joseph Petzval Lens Design Approach. *International Optical Design Conference 2017* (pp. 1-15). Denver, CO: Optica.
- Sasian, J. (2022). Lecture 15: Refractive Systems. Tucson, AZ: <https://wp.optics.arizona.edu/jsasian/courses/opti-518/>.
- Vasiljević, D. (2002). *Classical and Evolutionary Algorithms in the Optimization of Optical Systems*. Boston, MA: Springer.
- Xie, X., Fan, H., Wang, H., Wang, Z., & Zou, N. (2018). Error of the slanted edge method for measuring the modulation transfer function of imaging systems. *Applied Optics*, B83-B91.